Using (15)–(18) and the identities (21), (22), and

$$\nabla\cdot(\phi^*\boldsymbol{D})=\phi^*(\nabla\cdot\boldsymbol{D})+(\nabla\phi^*)\cdot\boldsymbol{D} \tag{39}$$

and the equation of continuity

$$\nabla\cdot\boldsymbol{D}=\rho_e \tag{40}$$

and applying the approach used in deriving the complex reciprocity theorem (27), we obtain the quasi-electrostatic form of the complex reciprocity theorems

$$P_s(a,b)=-P_s(b,a)^* \tag{41}$$

$$P_s(b,a)=-P_s(a,b)^* \tag{42}$$

where

$$P_s(a,b)=\int\int_R\int\{\boldsymbol{v}_b\cdot\boldsymbol{F}_a^*+\phi_b(j\omega\rho_{ea})^*\}\,dV \tag{43}$$

is the quasistatic complex mutual power and ρ_{ea} is the electric charge density of sources a.

References

[1] *IEEE Trans. Microwave Theory Tech.* (Special Issue on Microwave Acoustics), vol. MTT-17, Nov. 1969; also *IEEE Trans. Microwave Theory Tech.* (Special Issue on Microwave Accoustic Signal Processing), vol. MTT-21, Apr. 1973.

[2] B. A. Auld, "Application of microwave concepts to the theory of acoustic fields and waves in solids," *IEEE Trans. Microwave Theory Tech.*, vol. MTT-17, pp. 800–811, Nov. 1969.

[3] ——, *Acoustic Fields and Waves in Solids, Vol. 1 and Vol. 2.* New York: Wiley, 1973.

[4] M. Kobayashi, "Reciprocity theorem for a region with inhomogeneous anisotropic media and with surface impedance," *Proc. IEEE*, vol. 63, pp. 1245–1246, Aug. 1975.

[5] ——, "Reciprocity theorem for a region with inhomogeneous bianisotropic media and surface impedance," *IEEE Trans. Microwave Theory Tech.*, vol. MTT-24, Feb. 1976.

[6] R. F. Harrington, *Time-Harmonic Electromagnetic Fields.* New York: McGraw-Hill, 1961, p. 22.

Application of Generalized Characteristic Vectors to Problems of Propagation in Clad Inhomogeneous Dielectric Waveguides

EZEKIEL BAHAR, SENIOR MEMBER, IEEE, AND BISHAN S. AGRAWAL

Abstract—**A transformation matrix that uses generalized characteristic vectors is used to convert Maxwell's equations into a set of loosely coupled equations for the wave amplitudes. This transformation is suitable for permittivity profiles with turning points. In earlier full-wave solutions to these equations, several special functions that account for the local features of the permittivity profile, especially near the turning points, were used to obtain appropriate expansions of the fields.**

The transverse field components, the propagation coefficients, as well as the phase and group velocities, are computed for both horizontally polarized (TE) and vertically polarized (TM) modes of the dielectric waveguides using the full-wave approach. These solutions are compared with analytic solutions for waveguides with special permittivity profiles. They are also compared with recently published results based on a perturbational approach.

Manuscript received August 21, 1978; revised December 1, 1978. This work was supported in part by the National Science Foundation, the U.S. Army Research Office, and the Engineering Research Center of the University of Nebraska.

The authors are with the Department of Electrical Engineering, University of Nebraska, Lincoln, NE 68588.

I. Introduction

MAXWELL'S equations for the transverse electromagnetic field components in clad inhomogeneous dielectric waveguides are converted into loosely coupled sets of equations for the wave amplitudes. The nonsingular transformation matrix that is used to obtain the equations for the wave amplitudes consists of generalized characteristic vectors of rank one and two in order to account for wave coupling near the turning points [2]. Thus in this work no special functions are used to describe the fields near the turning points as was done in the previous work by the authors [3].

The full-wave approach presented here is applicable to clad or unclad dielectric waveguides with arbitrary permittivity profiles. It can be used in single-mode as well as in multimode waveguides.

For the illustrative examples presented, waveguides with special permittivity profiles that can be solved ana-

0018-9480/79/0400-0345$00.75 ©1979 IEEE

lytically in closed form are considered. Comparison with recently published solutions based on a perturbational approach [5] is also given.

Special consideration is also given in this paper to the dispersive properties of the dielectric waveguides. Thus the phase and group velocities are also computed as functions of frequency. Two parameters f_m and g_m which represent the deviation of the phase and group velocities of the waveguides from those of an ideal nondispersive waveguide are plotted as functions of frequency for several TE and TM modes of the guiding structure.

II. Formulation of the Problem

To demonstrate the versatility of the analytic techniques used in this work and to compare these results with recently published solutions based on a perturbational approach [5], we consider here both horizontally and vertically polarized waves in horizontally stratified dielectric media (see Figs. 1 and 2). Thus for the region of width L, the permittivity relative to free space is

$$\epsilon(z)/\epsilon_0 = n^2 = \begin{cases} n_0^2[1-\chi(z)], & -L/2 < z < L/2 \\ n_0^2[1-\chi(L/2)], & |z| > L/2 \end{cases} \tag{1}$$

where n_0 is the refractive index at the center of the slab. The permeability is μ_0 for all z. Assuming that all the fields are independent of y and suppressing the common factor $\exp(i\omega t)\exp(-iksx)$, the transverse (x,y) components of the electromagnetic field can be shown to satisfy the coupled differential equations [2]

$$\frac{de}{dv} \equiv e' = Te \tag{2}$$

where

$$e = \begin{bmatrix} E_x \\ -E_y \\ H_x \\ H_y \end{bmatrix} \qquad T = \begin{bmatrix} 0 & 0 & 0 & q^2/n^2 \\ 0 & 0 & 1 & 0 \\ 0 & q^2 & 0 & 0 \\ n^2 & 0 & 0 & 0 \end{bmatrix} \tag{3}$$

and

$$v - v_0 = -ik(z - z_0) \qquad q^2 = n^2 - s^2 \tag{4}$$

in which v_0 and z_0 are arbitrary constants, k is the free space wavenumber, and n is the refractive index. The propagation coefficient is $\beta = ks$; thus for $s < n$, s/n is the sine of the angle of the wave (with respect to the z axis) inside the dielectric. A nonsingular 4×4 transformation matrix S is used to express the fields e in terms of loosely coupled forward and backward traveling horizontally and vertically polarized wave amplitudes f:

$$e = Sf. \tag{5}$$

Thus the field equation (2) is transformed into

$$f' = S^{-1}(TS - S')f \equiv Cf \tag{6}$$

where $S' = dS/dv$. For the region centered about $z = z_c$, $|z - z_c| \leq \Delta z/2$, the transformation matrix S satisfies the equation

$$S^{-1}(T_c S - S') = \Delta_c \tag{7}$$

where $T_c = T(z_c)$ and the elements of the diagonal matrix Δ_c are the generalized characteristic values and the columns of the transformation matrix S can be expressed in terms of generalized characteristic vectors [2]. Thus when q_i, the characteristic values of the matrix T, are sufficiently distinct (away from turning points) in the region $|z - z_c| \leq \Delta z/2$, the constant transformation matrix S is

$$S = \begin{bmatrix} 0 & 0 & q_c/n^2 & -q_c/n^2 \\ 1 & 1 & 0 & 0 \\ q_c & -q_c & 0 & 0 \\ 0 & 0 & 1 & 1 \end{bmatrix} \tag{8}$$

$$\Delta_c = \begin{bmatrix} q_c & 0 & 0 & 0 \\ 0 & -q_c & 0 & 0 \\ 0 & 0 & q_c & 0 \\ 0 & 0 & 0 & -q_c \end{bmatrix} \tag{9}$$

and

$$C = \frac{1}{2q_c}\begin{bmatrix} q^2+q_c^2 & q^2-q_c^2 & 0 & 0 \\ -q^2+q_c^2 & -q^2-q_c^2 & 0 & 0 \\ 0 & 0 & (qn_c/n)^2+(q_cn/n_c)^2 & (qn_c/n)^2-(q_cn/n_c)^2 \\ 0 & 0 & -(qn_c/n)^2+(q_cn/n_c)^2 & -(qn_c/n)^2-(q_cn/n_c)^2 \end{bmatrix}. \tag{10}$$

Thus C reduces to the diagonal matrix Δ_c (9) at $z = z_c$:

$$C(z_c) = \Delta_c. \tag{11}$$

For critical coupling regions where $q^2 = n^2 - s^2 \to 0$, the transformation matrix (7) becomes singular. For these regions we use generalized characteristic vectors to define S [2]:

$$S = S_0 + S_1 = \begin{bmatrix} 0 & 0 & 0 & 0 \\ 1 & 1 & 0 & 0 \\ 0 & 0 & 0 & 0 \\ 0 & 0 & s^2 & s^2 \end{bmatrix} + \frac{1}{v}\begin{bmatrix} 0 & 0 & 0 & 1 \\ 0 & 0 & 0 & 0 \\ 0 & 1 & 0 & 0 \\ 0 & 0 & 0 & 0 \end{bmatrix} \tag{12}$$

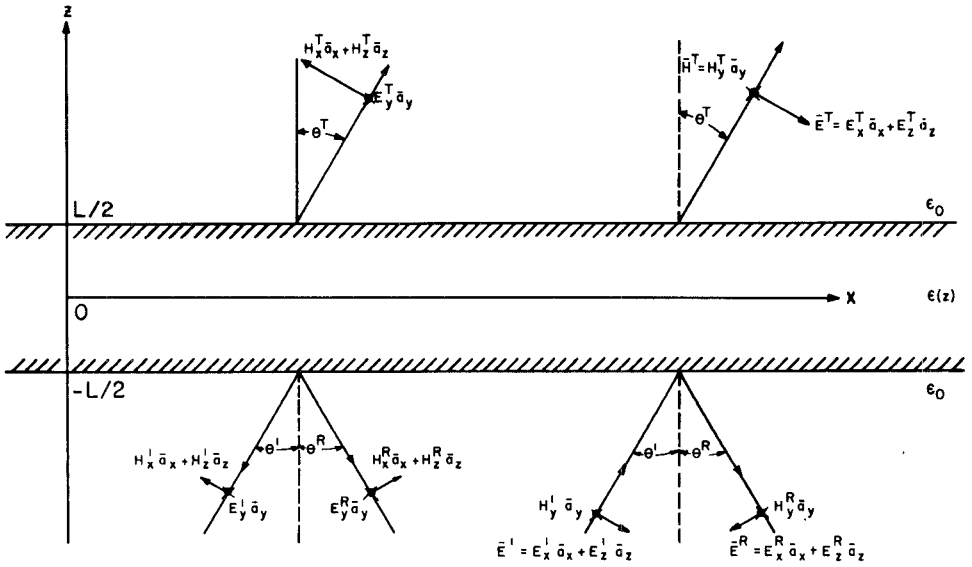

Fig. 1. Horizontally and vertically polarized waves in a horizontally stratified dielectric slab.

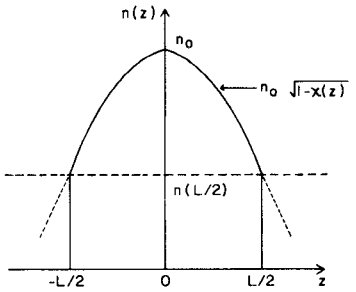

Fig. 2. Refractive index distribution of a clad inhomogeneous dielectric waveguide (solid lines). The dotted curve indicates the refractive index distribution for an ideal waveguide.

and

$$\Delta_c = \frac{1}{v}\begin{bmatrix} 0 & 0 & 0 & 0 \\ 0 & 1 & 0 & 0 \\ 0 & 0 & 0 & 0 \\ 0 & 0 & 0 & 1 \end{bmatrix}. \tag{13}$$

For the critical coupling regions $|z - z_c| \leq \Delta z/2$, S is a function of z and $S' \neq 0$, and C (6) is given by

$$C = v\begin{bmatrix} -q^2 & -q^2 & 0 & 0 \\ q^2 & q^2+1/v^2 & 0 & 0 \\ 0 & 0 & -(qs/n)^2 & (q/vs)^2-(qs/n)^2 \\ 0 & 0 & (qs/n)^2 & (qs/n)^2+1/v^2 \end{bmatrix}. \tag{14}$$

Thus at $z = z_c$, $q = 0$, and C reduces to the diagonal matrix Δ_c (13).

In view of the forms of the matrix C, (10) and (14), the generalized characteristic vectors are used to define S (12) for regions where

$$|q| \leq \epsilon_T = 10^{-2}. \tag{15}$$

For convenience we choose $v_0 = 0$ and $z_0 = z_c - L/4$ in (4). Since the transverse components of the electromagnetic fields are continuous for $-L/2 \leq z \leq L/2$, at the interface $z = z_T$ between two adjacent regions of width Δz

$$e(z_T) = S(z_T^-)f(z_T^-) = S(z_T^+)f(z_T^+) \tag{16}$$

where

$$z_T^{\pm} = \lim_{\delta \to 0} z_T \pm \delta, \qquad \delta > 0. \tag{17}$$

In free space, the transformation matrix S is given by (8) with $q_c^2 = n_c^2 - s^2$ replaced by $c^2 = 1 - s^2$.

The boundary conditions at $z = L^+/2$ for horizontally (TE) and vertically (TM) polarized waves are f^H and f^V, respectively, where

$$f^H(L^+/2) = \begin{bmatrix} 1 \\ 0 \\ 0 \\ 0 \end{bmatrix} \text{ and } f^V(L^+/2) = \begin{bmatrix} 0 \\ 0 \\ 1 \\ 0 \end{bmatrix}. \tag{18}$$

For the trapped waveguide modes of the structure, (6) is solved numerically for assumed values of s, using (15) as initial conditions. This yields the values for the wave amplitudes at $z = -L^-/2$, $f^H(-L^-/2)$, and $f^V(-L^-/2)$. Using the method of interval halving, we determine the values of s for which $f_1^H(-L^-/2) = 0$ and $f_3^V(-L^-/2) = 0$ for the horizontally and vertically polarized modes, respectively. For symmetric permittivity profiles, $\epsilon(z) = \epsilon(-z)$, the solutions may be simplified by noting that either E_y or H_x vanish at $z = 0$ for the horizontally polarized modes and either E_x or H_y vanish at $z = 0$ for the vertically polarized modes. The parameter s/n corresponds to the sine of the angles of the wave normal from the z axis. Thus the fields are expressed as propagating waves for regions where $s/n < 1$, $(q > 0)$ and evanescent waves for regions where $s/n > 1$, $(q = -i|q|)$. And for all

the trapped waveguide modes of the structure

$$n_0 > s > n(L/2). \tag{19}$$

For the horizontally stratified problem treated here, the horizontally and vertically polarized waves are uncoupled, and it is also possible to formulate the problem in terms of two independent pairs of coupled equations [3]. For single-mode dielectric waveguides ($L \simeq \lambda$), the Runge–Kutta method is suitable to solve the coupled equations for the wave amplitudes (6). However, for multimode structures ($L \simeq 100\lambda$), a recurrence formula, that has been derived after converting (6) into integral equations, is found to be more suitable for numerical computations than the Runge–Kutta method (see Appendix I).

III. Illustrative Examples

The analytic method outlined in this paper is suitable for arbitrary permittivity profiles $\epsilon(z)$, (1). However, for the purposes of comparison with earlier work, two special forms of the permittivity profile are considered in detail here. The first

$$n^2(z) = n_0^2/\cosh^2(gz) \tag{20}$$

was considered by Kornhauser and Yaghjian [6]. For the unclad case, ($L \to \infty$) exact closed form analytic solutions for the horizontally polarized modes can be written in terms of the associated Legendre functions. For this case the propagation coefficient β is given by

$$\beta^2 = k^2 s^2 = (\mu/g)^2, \qquad \mu = -\nu + m \ (m = 0, 1, 2, \cdots) \tag{21}$$

where m is the mode number, g is a constant, and

$$\nu(\nu+1) = (k/g)^2. \tag{22}$$

The second permittivity profile

$$n^2(z) = n_0^2\left(1 - \alpha(gz)^2 - \delta(gz)^3 - \gamma(gz)^4\right) \tag{23}$$

was considered by Hashimoto [4], [5] for the case $\delta = 0$. For the unclad case with $\delta = 0$ and $\gamma = 0$, exact closed form analytic solutions for the horizontally polarized modes can be written in terms of parabolic cylindrical functions. For this case $L \to \infty$, $\delta = \gamma = 0$:

$$\beta_m^2 = k^2 s_m^2 = k^2(1 - b_m), \qquad b_m = \frac{g}{k}(2m+1), \qquad m = 0, 1, \cdots. \tag{24}$$

In addition to determining the propagation coefficients β and the transverse electromagnetic fields as a function of z, the phase and group velocities v_p and v_g, respectively, are evaluated as functions of frequency:

$$v_{pm} = \omega/\beta_m = \omega/ks_m = c_0/s_m, \qquad c_0 = (\mu_0\epsilon_0)^{-1/2} \tag{25}$$

and

$$v_{gm} = d\omega/d\beta_m. \tag{26}$$

For an ideal nondispersive waveguide $v_{gm} = c_0/n_0 = v_0$ where v_0 is the velocity of light in a homogeneous medium with $n = n_0$. Thus for the ideal waveguide

$$\partial v_{gm}/\partial\omega = 0$$

$$\Delta v_{gm}/\Delta m = 0$$

$$\partial s_m/\partial\omega = \left(\frac{1}{v_{gm}} - \frac{1}{v_{pm}}\right)/k \tag{27}$$

and

$$\beta_m(\omega) = \beta_m(\omega_c) + (\omega - \omega_c)/v_0. \tag{28}$$

To observe the dispersive properties of the dielectric waveguide, it is convenient to plot the function

$$h_m(\omega) = (1 - s_m(\omega_c)/n_0)/(1 - s_m(\omega)/n_0) = (1 - v_0/v_{pm}(\omega_c))/(1 - v_0/v_{pm}(\omega)) \tag{29}$$

(ω_c is a fixed carrier frequency) as well as the normalized group velocity

$$g_m(\omega) = v_{gm}/v_0 - 1. \tag{30}$$

For the ideal waveguide v_{pm} is not constant, and h_m and g_m reduce to

$$h_{mI}(\omega) = \omega/\omega_c \text{ and } g_{mI}(\omega) = 0. \tag{31}$$

For all the illustrative examples presented in this paper,

$$n_0 = 1.53 \qquad g = 3.23 \text{ mm}^{-1} \qquad k = k_c = \frac{2\pi}{\lambda_c} = 10^4 \text{ mm}^{-1} \tag{32}$$

and the carrier frequency is $\omega_c = 3.10^{15} \text{ s}^{-1}$.

In Table I, the propagation coefficient β_m for clad and unclad dielectric waveguides with parabolic permittivity profiles $\alpha = 1$, $\delta = 0$, and $\gamma = 0$ in (24) are presented. They are computed using the full-wave technique presented in this paper. In addition, for the unclad case, $\beta_m = \beta_m^0$ is computed using the closed form analytic expression (24), and $\beta_m = \beta_m^c$ for the clad case with $L/2 = 12.6$ μm is computed using a perturbational method; thus

$$\beta_m^c/k = (1 - b_{\nu_m})^{1/2}, \qquad b_{\nu_m} = \frac{g}{k}(2\nu_m + 1) \tag{33}$$

where $\nu_m = m + \Delta\nu_m$ and $\Delta\nu_m$ is evaluated by Hashimoto [5]. The effects of cladding which are given by the parameter

$$\Delta\beta_m = (\beta_m^c - \beta_m^0) \tag{34}$$

become more significant as m (the mode number) increases. For $m = 3$, the two values for $\Delta\beta_m$ differ in the second significant figure.

In Table II, the propagation coefficient β_m for the clad and unclad near parabolic profile ($\alpha = 1$, $\delta = 0$, and $\gamma = 100$) is presented. Using the perturbational method for the unclad dielectric [4]

$$b_m = \frac{g}{k}(2m+1) + \left(\frac{g}{k}\right)^2 \gamma \frac{3}{4}(2m^2 + 2m + 1) - \left(\frac{g}{k}\right)^3 \gamma^2 \left[\frac{17}{64}(2m+1)^3 + \frac{67}{64}(2m+1)\right]. \tag{35}$$

TABLE I
VALUES OF β_m, $\Delta\beta_m$, and $\Delta\nu_m$ FOR n^2 (3.4) AND (3.5) WITH $\alpha=1$, $\delta=0$, $\gamma=0$

		m=0	m=1	m=2	m=3
β_m^0/k	c.	1.5298384915	1.529515423	1.52919229	1.5288691
	b.	1.5298384915	1.529515423	1.52919229	1.5288691
β_m^c/k	a.	1.5298385044	1.529515714	1.52919520	1.5288949
	b.	1.5298385051	1.529515711	1.52919526	1 5288908
$\Delta\beta_m$	a.	1.29×10^{-4}	2.91×10^{-3}	2.91×10^{-2}	2.59×10^{-1}
	b	1.37×10^{-4}	2.88×10^{-3}	2.97×10^{-2}	2.18×10^{-1}
$\Delta\nu_m$	a.	-0.4×10^{-4}	-0.9×10^{-3}	-0.9×10^{-2}	-0.8×10^{-1}
	b.	-0.42×10^{-4}	-0.89×10^{-3}	-0.92×10^{-2}	-0.67×10^{-1}

Superscript 0 is for unclad waveguide.
Superscript c is for clad waveguide with $L/2=12.6$ μm.
a. Data from Hashimoto [5].
b. Data using the full-wave formulation presented in this paper.
c. Data using exact analytic solution (24).

TABLE II
VALUES OF β_m, $\Delta\beta_m$, and $\Delta\nu_m$ FOR n^2 (3.4) AND (3.5) WITH $\alpha=1$, $\delta=0$, $\gamma=100$

		m=0	m=1	m=2	m=3
β_m^0/k	a.	1.529836029	1.529503376	1.52916180	1.5288122
	b.	1.529836022	1.529503297	1.52916141	1.5288110
β_m^c/k	a.	-----	-----	-----	1.5288249
	b.	1.529836032	1.529503498	1.52916336	1.5288242
$\Delta\beta_m$	a.	-----	-----	-----	1.27×10^{-1}
	b.	1.03×10^{-4}	2.01×10^{-3}	1.96×10^{-2}	1.33×10^{-1}

Superscript 0 is for unclad waveguide.
Superscript c is for clad waveguide with $L/2=12.6$ μm.
a. Data from Hashimoto. ($\Delta\nu_3 \simeq -0.36\times10^{-1}$)
b. Data using the full-wave formulation presented in this paper.

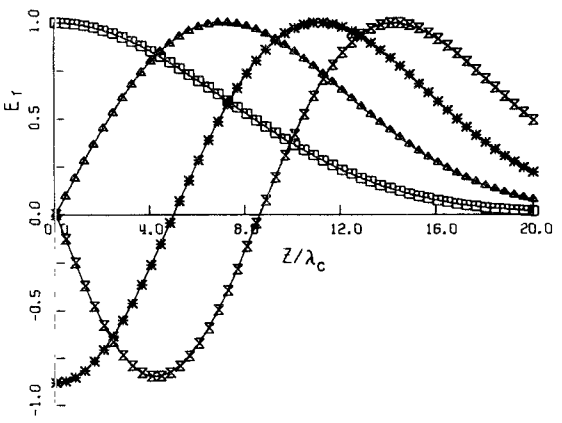

Fig. 3. Electric field component E_y for TE_m modes for $\alpha=1$, $\delta=0$, $\gamma=100$, and $L=126\lambda/\pi$ ($m=0$ (□), $m=1$ (△), $m=2$ (*), and $m=3$ (X)).

For the clad case [5], m in (35) is replaced by $\nu_m=m+\Delta\nu_m$. In an earlier comparison of the full-wave solutions with the perturbational solutions, it was shown that, except for $m=0$, the perturbational solution for the near parabolic profile is less accurate than the familiar WKB

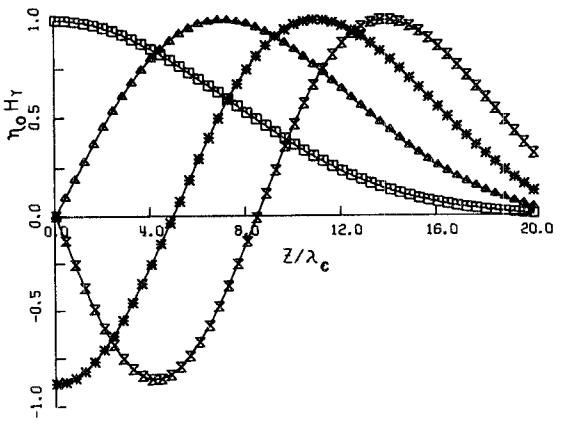

Fig. 4. Magnetic field component H_y for TM_m modes for $\alpha=1$, $\delta=0$, $\gamma=100$, and $L=126\lambda/\pi$ ($m=0$(□), $m=1$ (△), $m=2$ (*), and $m=3$ (X)).

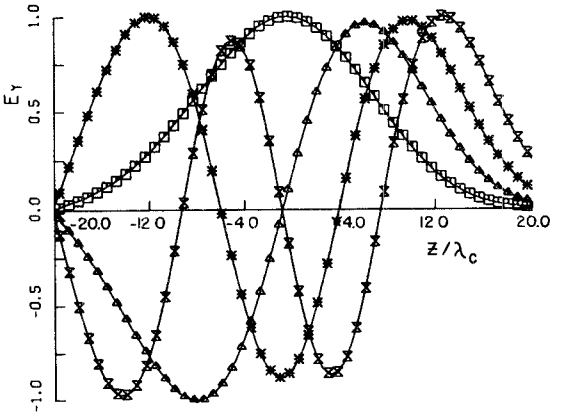

Fig. 5. Electric field component E_y for TE_m modes for $\alpha=1$, $\sigma=10$, $\gamma=100$, and $L=126\lambda/\pi$ ($m=0$(□), $m=1$ (△), $m=2$ (*), and $m=3$ (X)).

solutions [3]. The perturbational solution for the clad near parabolic permittivity profile is given only for mode $m=3$.

In Fig. 3, the electric field $\bar{E}=\bar{a}_y E_y$ is plotted as a function of z/λ_c for the first four TE_m modes, and in Fig. 4, the magnetic field $\bar{H}=\bar{a}_y H_y$ is plotted for the first four TM_m modes. In both Figs. 3 and 4, the near parabolic permittivity profile is considered.

In Fig. 5, the electric field for the first four TE_m modes is plotted for a waveguide with a nonsymmetric permittivity profile ($\alpha=1$, $\delta=10$, and $\gamma=100$ in (23)). Since $\delta>0, n^2(z)<n^2(-z)$, more power is distributed in the region $z<0$ than in the region $z>0$.

In Fig. 6, the electric field for the first four TE_m modes is plotted for a dielectric waveguide with a hyperbolic cosine permittivity profile (20). For this profile v_g is frequency dependent but independent of mode number.

In Figs. 7 and 8, h_m (29) and g_m (30) are plotted as functions of frequency for the clad and unclad parabolic profiles to show the effects of cladding on the phase and the group velocities. The first four TE_m and the first four TM_m modes are considered.

In Figs. 9 and 10, h_m and g_m are plotted for the near parabolic profile, and in Figs. 11 and 12, h_m and g_m are plotted for the hyperbolic cosine profile. Note that $\Delta v_g/\Delta m=0$ only for the unclad TE_m modes.

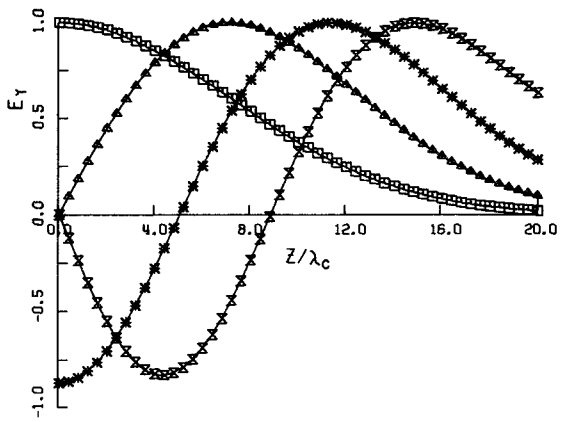

Fig. 6. Electric field component E_y for TE_m modes for hyperbolic cosine profile, and $L=126\lambda/\pi$ ($m=0$ (□), $m=1$ (△), $m=2$ (*), and $m=3$ (X)).

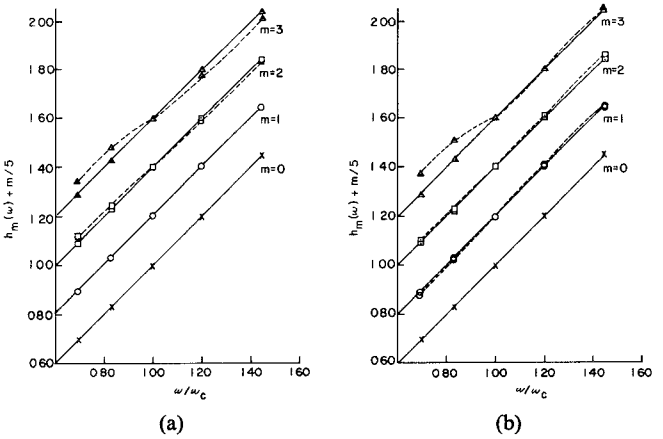

Fig. 7. Effects of cladding on phase velocity v_{pm} for $\alpha=1$, $\delta=0$, and $\gamma=0$. (a) TE_m modes, and (b) TM_m modes. Solid lines (——) are for unclad waveguides, and broken lines (---) are for clad waveguides.

The unclad waveguides with the parabolic profiles and the hyperbolic cosine profiles were considered here in particular because, for these waveguides, exact analytic solutions for the propagation coefficients are known and because of their special dispersive features. The full-wave solutions presented here are shown to be in full agreement with the analytic solution.

The full-wave approach is not restricted to waveguides with special permittivity profiles. To check the accuracy of the full-wave solutions for the near parabolic profiles ($\delta\neq,\gamma\neq0$) and for all the unclad cases considered, the differential equations for the transverse field components (3) have also been integrated numerically. These results are also in excellent agreement with the full-wave solution (up to 12 significant figures for β_m).

IV. Concluding Remarks

The full-wave approach based on the use of a nonsingular transformation matrix consisting of generalized characteristic vectors is shown to provide very accurate solutions for the TE and TM modes of clad dielectric waveguides with arbitrary permittivity profiles. It does not employ a series of special functions to determine the behavior of the fields near the turning points where the forward and the backward propagating waves become evanescent. Furthermore, unlike the perturbational methods, for the full-wave approach, it is not necessary to know the exact analytical solutions for a permittivity profile that very closely resembles the permittivity profile under consideration [3]. The full-wave approach can be used to determine the fields of single-mode and multimode structures. When the width of the dielectric waveguide is much larger than the wavelength in the medium, a recursive solution to the coupled wave equations (given in Appendix I) has been found to be more suitable than the familiar Runge–Kutta solution [1], especially for the higher order modes. The computations were executed on an IBM 360/65 computer. The execution time for determining a set of four roots s_m (using an interval halving technique) is about 3 min with $L>126\lambda_c/\pi$.

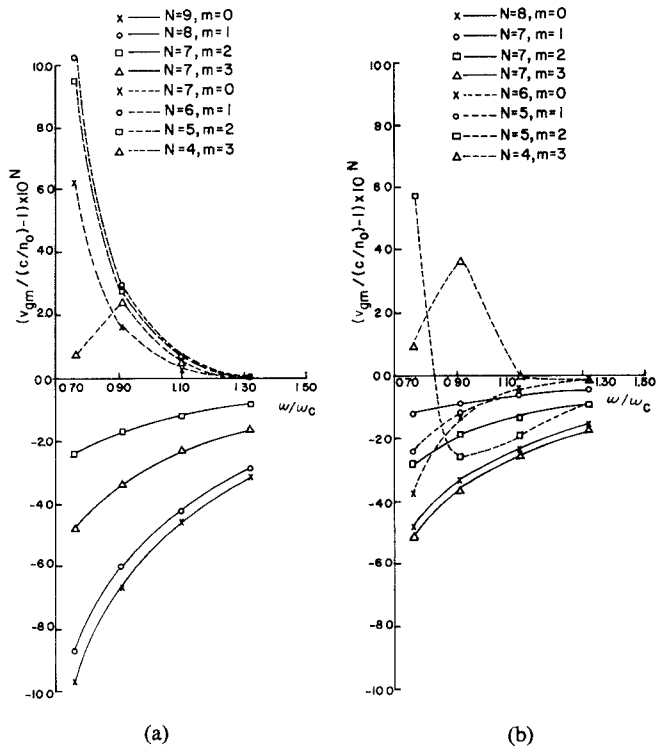

Fig. 8. Variation in group velocity v_{gm} for unclad (——) and clad (---) dielectric waveguides for $\alpha=1$, $\delta=0$, and $\gamma=0$. (a) TE_m modes, and (b) TM_m modes. Note: N is a scaling factor.

The dispersive properties of the waveguides are presented by the parameters $h_m(\omega)$ (29) and $g_m(\omega)$ (30) that are related to the phase and group velocities. A comparison of these quantities with those of an ideal nondispersive multimode waveguide is presented for several TE and TM modes in clad waveguides with three different permittivity profiles. The variation of the function $g_m(\omega)$ is larger for clad waveguides than for unclad waveguides, and these variations usually increase with mode number m. It is interesting to point out that, in general, $g_m(\omega)$ can be positive or negative. Thus the group velocity can be larger

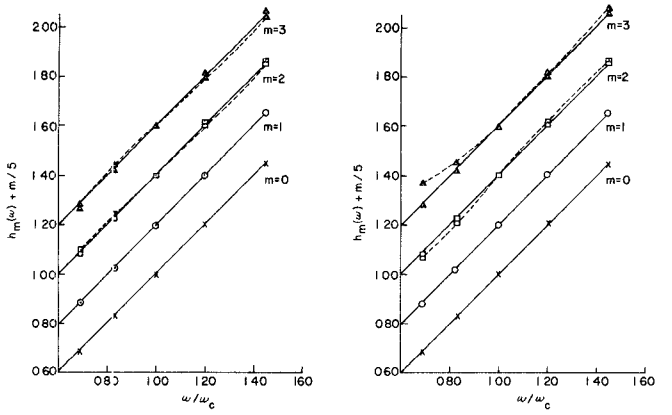

Fig. 9. Effects of cladding on phase velocity v_{pm} for $\alpha=1$, $\sigma=0$, and $\gamma=100$. (a) TE_m modes, and (b) TM_m modes. Solid lines (——) are for unclad waveguides, and broken lines (---) are for clad waveguides.

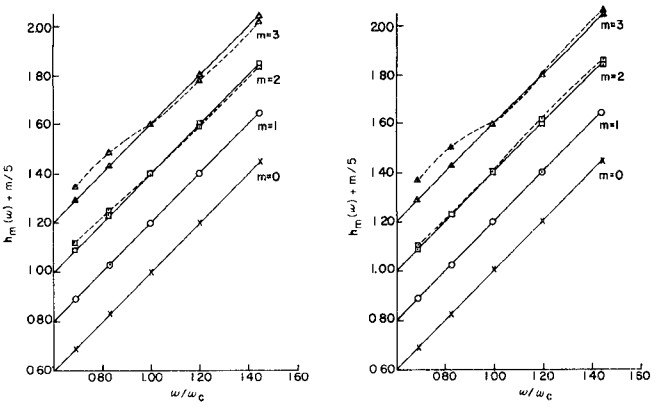

Fig. 11. Effects of cladding on phase velocity v_{gm} for a hyperbolic cosine permittivity profile. (a) TE_m modes, and (b) TM_m modes. Solid lines (——) are for unclad waveguides, and broken lines (---) are for clad waveguides.

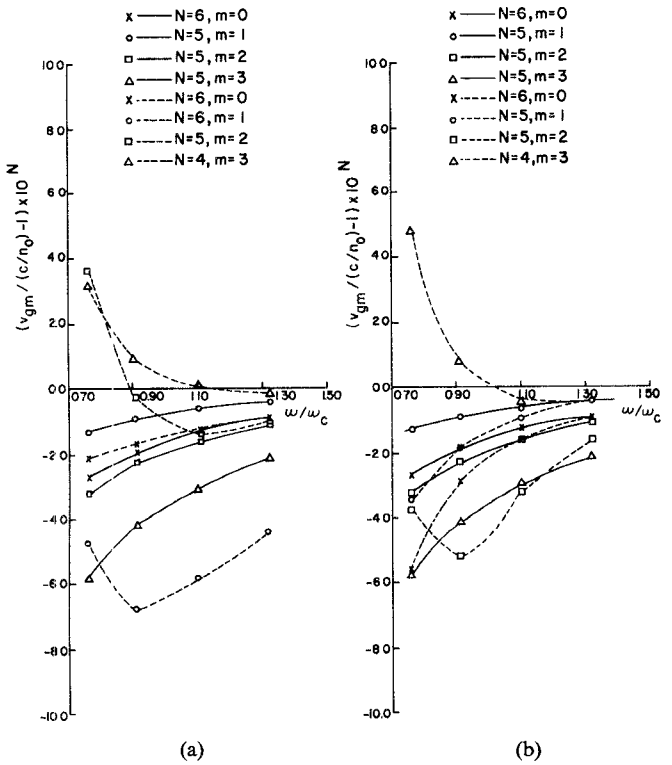

Fig. 10. Variation in group velocity v_{gm} for unclad (——) and clad (---) dielectric waveguides for $\alpha=1$, $\delta=0$, and $\gamma=100$. (a) TE_m modes, and (b) TM_m modes. Note: N is a scaling factor.

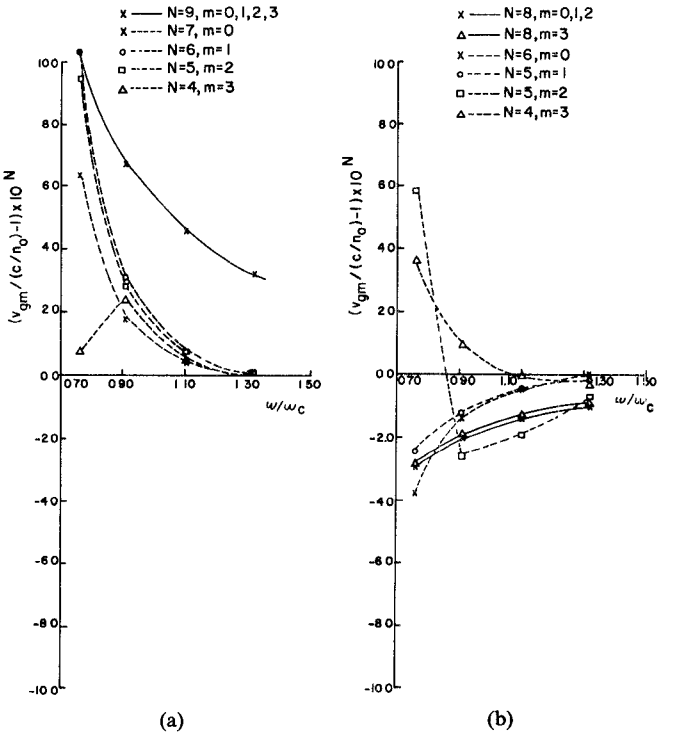

Fig. 12. Variation in group velocity v_{gm} for unclad (——) and clad (---) dielectric waveguides for a hyperbolic cosine permittivity profile. (a) TE_m modes, and (b) TM_m modes. Solid lines (——) are for unclad waveguides, and broken lines (---) are for clad waveguides. Note: N is a scaling factor.

or smaller than the velocity of light in a homogeneous medium with relative permittivity $n(0)=n_0$. For some clad waveguides, g_m vanishes at some point within the frequency range considered.

The method described here, using generalized characteristic vectors, could also be applied to dielectric waveguides with circular cross sections. In this case, however, the solutions cannot be expressed in terms of TE and TM modes, and all the four transverse components of the electromagnetic fields are coupled.

Appendix I

The coupled differential equation (6) can be expressed as the following integral equations:

$$f_m(z)=f_m(z_T)\exp\int_{z_1}^{z}C_{mm}(z')dz' + \int_{z_1}^{z}\Big[\sum_n{}'C_{mn}(z')a_n(z')\exp\int_{z'}^{z}C_{mm}(u)du\Big]dz' \quad \text{(A1)}$$

where the symbol Σ'_n implies that the summation does not include $n=m$. On replacing the coefficients $C_{mn}(z')$ by the first three terms of its Taylor series expansion, a recurrence formula that expresses $f_m(z-\Delta z)$ in terms of $f_m(z)$ is obtained upon integration. Thus the solution of (A1) for the region $z_T > z > z_B$ is

$$f_m(p+1) = P_m^-(p+1/2)\left[f_m(p)P_m^+(p+1/2) + \sum_n{}' D_{mn}(p+1/2) f_n(p) P_n^+(p+1/2)\right] \quad \text{(A2)}$$

where

$$z_T = L - p\Delta z,$$
$$z_B = L - (p+1)\Delta z,$$
$$z_c = L - (p+1/2)\Delta z \quad \text{(A3)}$$

$$P_m^{\pm} = \exp\left[-\frac{\Delta z}{2}\left\{ C_{mn} \pm \frac{\Delta z}{4} C'_{mn} + \frac{(\Delta z)^2}{24} C''_{mm} \right\}\right] \quad \text{(A4)}$$

$$D_{mn} = -\Delta z \operatorname{sinc} \theta_{mn}\left[C_{mn} + \frac{i\Delta z}{2} C'_{mn} \frac{1-\theta_{mn}\cot\theta_{mn}}{\theta_{mn}} + \frac{(\Delta z)^2}{8} C''_{mn}\left\{ 1 - \frac{2(1-\theta_{mn}\cot\theta_{mn})}{\theta_{mn}^2}\right\}\right] \quad \text{(A5)}$$

and

$$\theta_{mn} = \frac{i\Delta z}{2}\left[C_{mm} - C_{nn}\right]. \quad \text{(A6)}$$

Acknowledgment

The authors wish to thank Mrs. E. Everett for typing the manuscript.

References

[1] M. Abramowitz and I. A. Stegun, *Handbook of Mathematical Functions with Formulas, Graphs and Mathematical Tables* (Applied Mathematics Series 55). Washington, DC: National Bureau of Standards, U.S. Government Printing Office, 1964.

[2] E. Bahar, "Generalized characteristic functions for simultaneous linear differential equations with variable coefficients applied to propagation in inhomogeneous anisotropic media," *Can. J. Phys.*, vol. 54, no. 3, pp. 301–316, 1976.

[3] E. Bahar and B. S. Agrawal, "A generalized WKB approach to propagation in inhomogeneous dielectric waveguides," *Radio Sci.*, vol. 12, no. 4, pp. 611–618, 1977.

[4] M. Hashimoto, "A perturbational method for the analysis of wave propagation in inhomogeneous dielectric waveguides with perturbed media," *IEEE Trans. Microwave Theory Tech.*, vol. MTT-24, pp. 559–566, 1976.

[5] ——, "Propagation of cladded inhomogeneous dielectric waveguides," *IEEE Trans. Microwave Theory Tech.*, vol. MTT-24, pp. 404–409, 1976.

[6] E. T. Kornhauser and A. D. Yaghjian, "Modal solution of a point source in a strongly focusing medium," *Radio Sci.*, vol. 2, no. 3, pp. 299–310, 1967.

Modal Analysis of Homogeneous Optical Fibers with Deformed Boundaries

EIKICHI YAMASHITA, MEMBER, IEEE, KAZUHIKO ATSUKI, OSAMU HASHIMOTO, AND KOUJI KAMIJO

***Abstract*—The modal characteristics of homogeneous optical fibers with several types of deformed boundaries are analyzed by a numerical method based on the point-matching principle. The propagation constants of various modes are given. The separation of degeneracy in the dominant mode is discussed. The results of microwave-model experiments show good agreement with those of calculation.**

Manuscript received March 16, 1978; revised August 22, 1978.

E. Yamashita and K. Atsuki are with the University of Electro-Communications, Tokyo, Japan.

O. Hashimoto is with Tokyo Shibaura Electric Company, Ltd., Tokyo, Japan.

K. Kamijo is with the Japan Broadcasting Corporation.

I. Introduction

With the recent development of communication techniques using low-loss optical fibers, it became important to investigate detailed electromagnetic fields and propagation characteristics of various optical fibers. We pay attention to modal characteristics of a class of optical fibers with deformed boundaries which would be caused in the process of fabrication. Many approximate methods have been recently applied to analyze graded index optical fibers. Yet, only a few papers have discussed the problem of deformed boundaries.

0018-9480/79/0400-0352$00.75 ©1979 IEEE